

Structure of copper(II) complexes with L-leucyl-D- or L-leucyl-L-phenylalanine and molecular orbital calculations on their stabilization

Giuseppe Maccarrone,^a Giorgio Nardin,^b Lucio Randaccio,^b Giovanni Tabbi,^a Marzio Rosi,^c Antonio Sgamellotti,^c Enrico Rizzarelli^{a,d} and Ennio Zangrando^b

^a Dipartimento di Scienze Chimiche, Università di Catania, 95125 Catania, Italy

^b Dipartimento di Scienze Chimiche, Università di Trieste, 34127 Trieste, Italy

^c Dipartimento di Chimica, Università di Perugia, 06100 Perugia, Italy

^d Istituto per lo studio delle Sostanze Naturali di Interesse Alimentare e Chimico Farmaceutico, 95125 Catania, Italy

The complexes $[\text{CuL}(\text{H}_2\text{O})]\cdot\text{H}_2\text{O}$ **1** ($\text{H}_2\text{L} = \text{L-Leu-D-Phe}$) and $[\text{CuL}]$ **2** ($\text{H}_2\text{L} = \text{L-Leu-L-Phe}$) have been prepared and structurally characterized. In both the co-ordination of the Cu is a distorted square pyramid with the dipeptide occupying three basal positions, the fourth being occupied by a carboxyl oxygen of an adjacent molecule. A water molecule and a peptide oxygen of another complex complete the co-ordination of copper in the apical position in **1** and **2**, respectively. Thus, the dipeptide acts also as a bridging ligand between the metal centres so that both compounds exhibit a polymeric structure in the solid state. In both the phenyl group of the dipeptide is far apart from the metal, since it is on the same side as the apical ligand. In contrast, an interaction between the phenyl residue with Cu in **2** is found in solution. The behaviour is interpreted as due to breaking of the polymeric structure detected in the crystal. The interaction between the copper(II) ion and the aromatic ring is evaluated by means of a molecular orbital approach carried out on the simplified model $[\text{Cu}(\text{OH})_2(\text{NH}_3)_2]$ interacting with a benzene molecule.

The thermodynamic stereoselectivity of copper(II) and palladium(II) complexes with respect to diastereoisomeric dipeptides has recently been explained, suggesting an interaction between the side-chain residues and/or between the metal ion and the dipeptide aromatic groups.^{1–5} In particular, it has been hypothesized that a direct interaction between the d electrons of the metal ion and the π -ring system, advocated on the basis of the spectroscopic data in solution,^{6–10} could decrease the solvophobic¹¹ or, in more classical terms, hydrophobic¹² interaction between the two side chains.²

The non-covalent interaction between a cation and a Π face of an aromatic structure can be regarded as an attraction between a positive charge and the quadrupole moment of the aromatic ring. These interactions play a significant role in a great variety of biological macromolecules.¹³

X-Ray structural studies on metal complexes of amino acids or peptides, containing aromatic side chains, showed two different behaviours. When the amino acid or dipeptide acts as a chelate bidentate ligand^{5,10,14–16} the side-chain residues occupy the space above the co-ordination plane with a metal–aromatic ring distance of *ca.* 3.0–3.3 Å, which is less than the van der Waals distance. On the contrary, when the dipeptide acts as a chelate tridentate ligand to the same metal centre^{5,17–19} the side aromatic group is significantly far apart from the metal, the shortest distance being about 3.45 Å.

Furthermore, a CD magnitude anomaly was observed for ternary copper(II) complexes involving an aromatic amino acid and glycine. This was assumed to be due to a possible attractive interaction between Cu^{II} and the aromatic ring.²⁰ Kim and Martin⁸ studied the ternary complex formation in various palladium–dipeptide–amine systems and evaluated the stability enhancement in $-\Delta G^\circ$ involved in the palladium(II)–aromatic ring and ligand–ligand interactions, on the basis of the stability constant values, being 0.3–1.5 and 2.6–3.8 kJ mol⁻¹ for palladium(II)–aromatic and phenyl–aromatic amine ring interactions, respectively.

In order to obtain further insight into the presence of weak

metal–aromatic ring interactions in solution and in the solid state (and whether these interactions are important factors for the conformation of the aromatic side chains in metal complexes) we synthesized and studied the copper(II) complexes with L-leucyl-L- and with L-leucyl-D-phenylalanine. The presence of interactions between the copper(II) ion and the aromatic ring was evaluated by means of theoretical calculations carried out on the simplified model $[\text{Cu}(\text{OH})_2(\text{NH}_3)_2]$ interacting with a benzene system.

Results and Discussion

Crystal and molecular structures

A view of the molecular complex **1**, together with the atom labelling scheme for non-H atoms, is shown in Fig. 1. The crystal structure, projected along the *c* axis, is in Fig. 2, and may be described as being built by ribbons of $[\text{CuL}(\text{H}_2\text{O})]$ units, ($\text{H}_2\text{L} = \text{L-Leu-D-Phe}$) held together by the phenylalanine carboxyl atom O(2) which co-ordinates to the copper atom of another unit along the *b* axis. These chains are bridged by the crystallization water molecule O(5), through hydrogen bonds with O(3) [2.771(4) Å] of the Leu residue of one chain and with the Cu-co-ordinated O(4) [2.787(5) Å] of the adjacent chain (Fig. 2). The co-ordination of the Cu atom is a distorted square pyramid with the dipeptide occupying three basal positions through the nitrogen atoms N(1) and N(2) and the carboxyl atom O(1) of the Phe residue. The fourth basal position is occupied by the O(2) atom of the neighbouring unit (at $-x, \frac{1}{2} + y - 1, -z + 1$, see above). The oxygen O(4) of a water molecule completes the square pyramid. The four basal donors are coplanar within ± 0.06 Å, with the copper atom displaced by 0.18 Å from their mean plane towards the apical O(4) donor. The basal Cu–N and Cu–O bond lengths agree well with those reported for other copper(II) peptide complexes.^{17,18,22,23} A selection of the bond lengths and angles occurring at the copper atom is given in Table 1. The geometry of the dipeptide ligand is

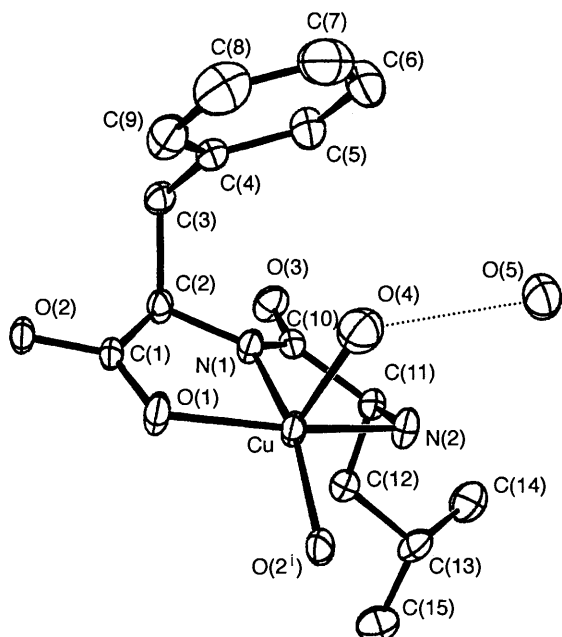


Fig. 1 An ORTEP²¹ drawing and atom numbering scheme of complex **1** (50% probability thermal ellipsoids); O(2ⁱ) pertains to the unit at $-x, \frac{1}{2} + y - 1, -z + 1$

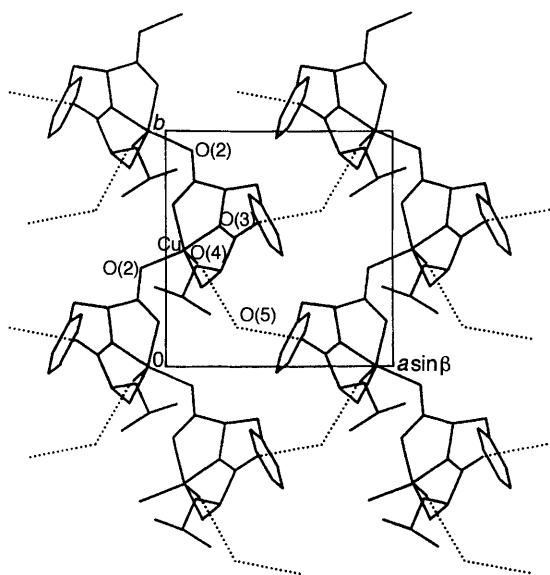


Fig. 2 Molecular packing of compound **1** viewed along the crystallographic *c* axis. Dotted lines indicate hydrogen bonds

such that the phenyl group is oriented on the side of the apical water molecule (Fig. 1), provoking widening of the N(1)–Cu–O(4) angle to 106.6(1)° (Table 1). This arrangement is similar to that found in the crystal structure of [CuL(H₂O)]·2H₂O (H₂L = L-Leu-L-Tyr).¹⁹ Intramolecular distances involving Cu and the phenyl group are larger than 4.0 Å, if Cu...C(4) 3.937(6) Å is excluded.

The ORTEP drawing of complex **2** is depicted in Fig. 3, together with the atom numbering scheme. The layered nature is shown in Fig. 4. The layer is built up by [CuL] (H₂L = L-Leu-L-Phe) units held together by the co-ordination of the carboxyl atom O(2) of one unit to the copper atom of the following unit, along the *b* axis, to form chains that are very similar to those of **1**. These chains, in turn, are linked side by side through the co-ordination of O(3) of each unit to a copper of the adjacent chain. The dipeptide co-ordinates by occupying the basal positions of a distorted square pyramid through the N(1), N(2) and O(1) donors, the fourth position being occupied by the oxygen O(2) of another CuL unit, as already observed in

Table 1 Co-ordination bond lengths (Å) and angles (°) for compounds **1** and **2**

1		2	
Cu–O(1)	2.009(2)	Cu–O(1)	2.014(4)
Cu–O(2 ⁱ)	1.974(2)	Cu–O(2 ⁱ)	1.977(4)
Cu–O(4)	2.282(3)	Cu–O(3 ⁱⁱ)	2.284(4)
Cu–N(1)	1.899(3)	Cu–N(1)	1.895(5)
Cu–N(2)	2.022(4)	Cu–N(2)	1.997(5)
O(1)–Cu–O(2 ⁱ)	93.0(2)	O(1)–Cu–O(2 ⁱ)	94.5(2)
O(1)–Cu–O(4)	92.7(1)	O(1)–Cu–O(3)	100.1(2)
O(1)–Cu–N(1)	81.9(1)	O(1)–Cu–N(1)	82.9(2)
O(1)–Cu–N(2)	163.3(1)	O(1)–Cu–N(2)	166.2(3)
O(2 ⁱ)–Cu–O(4)	87.3(2)	O(2 ⁱ)–Cu–O(3 ⁱⁱ)	84.0(2)
O(2 ⁱ)–Cu–N(1)	165.4(1)	O(2 ⁱ)–Cu–N(1)	161.7(2)
O(2 ⁱ)–Cu–N(2)	101.3(1)	O(2 ⁱ)–Cu–N(2)	97.7(3)
O(4)–Cu–N(1)	106.6(1)	O(3 ⁱⁱ)–Cu–N(1)	114.4(2)
O(4)–Cu–N(2)	96.7(1)	O(3 ⁱⁱ)–Cu–N(2)	87.7(3)
N(1)–Cu–N(2)	82.1(1)	N(1)–Cu–N(2)	83.7(2)

Symmetry transformations: **1**, $i - x, \frac{1}{2} + y - 1, -z + 1$; **2**, $i - x, \frac{1}{2} + y - 1, \frac{1}{2} - z$; $ii x - 1, y, z$.

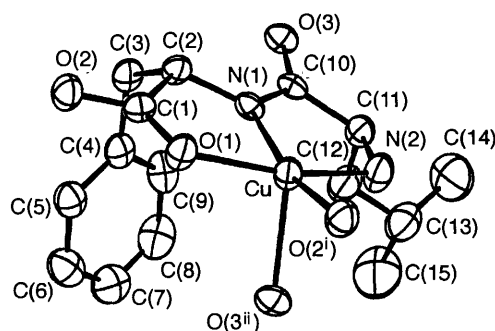


Fig. 3 An ORTEP drawing and atom numbering scheme of complex **2** (50% probability thermal ellipsoids); O(2ⁱ) and O(3ⁱⁱ) pertain to the units at $-x, \frac{1}{2} + y - 1, \frac{1}{2} - z$ and $x - 1, y, z$, respectively

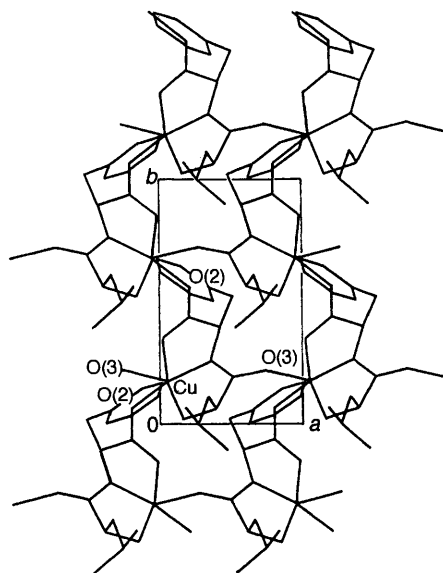


Fig. 4 Molecular packing of compound **2** viewed along the crystallographic *c* axis

the diastereoisomer **1**. The O(3) atom of a third unit coordinates to the copper in the apical position. The four nearest donors are coplanar within ± 0.13 Å and the metal is displaced from their mean plane by 0.19 Å, towards O(3).

The co-ordination bond lengths and angles (Table 1) have a similar trend in both complexes. The axial Cu–O(4) bond distance in complex **1** [2.282(3) Å] and Cu–O(3ⁱⁱ) in **2** [2.284(4) Å]

are close to those reported in similar five-co-ordinated square-pyramidal complexes $[\text{CuL}(\text{H}_2\text{O})]\cdot 2\text{H}_2\text{O}$ ($\text{H}_2\text{L} = \text{L-Leu-L-Tyr}$)¹⁹ and $[\text{CuL}(\text{H}_2\text{O})_2]$ ($\text{H}_2\text{L} = \text{Gly-L-Tyr}$).^{24,25} However, in complex **2**, more significant angular distortions are observed. The $\text{N}(1)\text{-Cu-O}(3^{\text{ii}})$ [$114.4(2)^\circ$] and $\text{O}(1)\text{-Cu-O}(3)$ [$100.1(2)^\circ$] angles are, in fact, noticeably larger than the corresponding $\text{N}(1)\text{-Cu-O}(4)$ [$106.6(1)^\circ$] and $\text{O}(1)\text{-Cu-O}(4)$ [$92.7(1)^\circ$] angles in **1**. On the other hand, the $\text{N}(2)\text{-Cu-O}(3^{\text{ii}})$ angle in **2** is about 10° smaller than the corresponding $\text{N}(2)\text{-Cu-O}(4)$ angle in **1**. Such distortions should be attributed, in both complexes, to the interaction of the phenyl group with the apical ligand (Figs. 1 and 3). In fact, the dipeptide co-ordinates in such a way that the phenyl ring is oriented on the side of the apical oxygen atom. In complex **2** the approach of the aromatic ring to the metal centre is such that the shortest intramolecular contact is $4.225(6) \text{ \AA}$ [$\text{Cu}\cdots\text{C}(4)$], slightly longer than the corresponding non-bonded interaction in **1**. On the contrary, in two square-pyramidal complexes $[\text{CuL}(\text{L}')]\text{ClO}_4$ [$\text{L} = \text{imidazole-4-ethanamine}$ (histamine), $\text{HL}' = \text{Phen}$ or Tyr]²³ and in $[\text{CuL}(\text{phen})]\text{-ClO}_4$ ($\text{HL} = \text{L-tryptophan}$, $\text{phen} = 1,10\text{-phenanthroline}$),¹⁶ the side-chain aromatic rings of the amino acids exhibit short contacts ($3.14\text{--}3.20 \text{ \AA}$) with the metal ion, most likely favoured by the stacking interactions with the co-ordinated diamines (namely histamine and phen).

Circular dichroism spectra

Complexes **1** and **2** in aqueous solution exhibit a specular behaviour both in the visible and the UV-region. Complex **2** shows a more negative maximum, however, due to the d-d transition, near 640 nm and a more positive maximum, which is generally ascribed to the charge-transfer between aromatic and aliphatic residues in complexes, near 330 nm ^{10,26} at pH 6.5. The spectra are shown in Fig. 5 and the corresponding data are in Table 2.

Absorption spectra

The absorption spectra in solution and in the solid state did not show any appreciable differences. However, in the solid state the interaction between the side-chain residue in the copper(II)

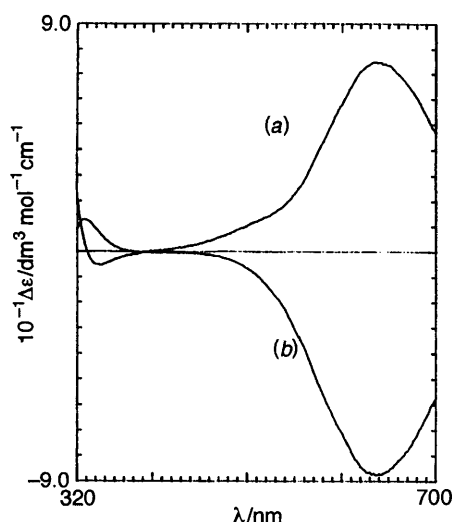


Fig. 5 The CD spectra of complexes **1** (a) and **2** (b)

Table 2 Circular dichroism spectral parameters for complexes **1** and **2** at pH 6.5

Complex	$\lambda_{\text{max}}/\text{nm}$ ($\Delta\epsilon/\text{dm}^3 \text{ mol}^{-1} \text{ cm}^{-1}$)
1	346 (0.0531), 640 (0.746)
2	328 (0.1267), 640 (0.870)

complex with the L-Leu-L-Phe dipeptide does not occur. This different behaviour may be due to breaking of the polymeric structure (Figs. 2 and 4) in solution. This might imply a complete rearrangement of the co-ordination about Cu, with formation of species where the dipeptide acts as a bidentate chelate ligand. This hypothesis is suggested by the observation that when dipeptides act as bidentate ligands their aromatic side groups are located above the metal at relatively short $\text{Cu}\cdots\text{C}$ contacts.^{5,10,14-16}

Copper-phenyl interaction

In order to understand whether the absence of an interaction between the copper atom and the phenyl group in the solid state is due to steric hindrance or to electronic effects, we performed *ab initio* calculations on the simplified model system $[\text{Cu}(\text{OH})_2(\text{NH}_3)_2(\text{C}_6\text{H}_6)]$. This system cannot present steric hindrance between copper and the aromatic ring because of the absence of the apical ligand.

Table 3 shows the total energy of $[\text{Cu}(\text{OH})_2(\text{NH}_3)_2(\text{C}_6\text{H}_6)]$, together with the total energies of the separated fragments. The distance between the copper atom and the centroid of the aromatic ring, keeping the latter parallel to the basal plane, was first optimized and a local minimum at a distance of 3.50 \AA was found. From the values in Table 3, however, it can be seen that this structure is unbound with respect to the optimized geometry fragments. A different situation arises if a bending of the benzene molecule with respect to the mean plane of the copper fragment is allowed. The simultaneous optimization of these two parameters led to a distance between the copper centre and the centroid of C_6H_6 of 3.57 \AA and to an angle between the C_6H_6 and the basal plane of 49.0° , with the benzene molecule bent towards the OH^- ligands. Close contacts between the copper ion and the aromatic ring are present in this optimized structure, the shortest distance being $r[\text{Cu}\cdots\text{C}(1)] = 2.85 \text{ \AA}$. This distance is slightly shorter than those reported for complexes in the solid state.^{10,12,18,23}

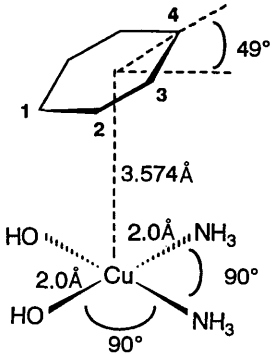
The binding energy between $[\text{Cu}(\text{OH})_2(\text{NH}_3)_2]$ and C_6H_6 is computed to be 11.2 kJ mol^{-1} , as can be deduced from the energies in Table 3. This value, though needing to be corrected for basis set incompleteness and correlation effects, suggests, however, the presence of an attractive interaction between the copper fragment and the benzene molecule. The analysis of the wavefunction, together with the Mulliken population analysis, (results in Table 4), shows that this interaction is essentially electrostatic and arises mainly from the interaction between the positively charged copper centre and the benzene π -electron density. This is in agreement with the results of previous calculations performed for other complexes involving intramolecular aromatic ring-stacking interactions.^{16,26} Table 4 shows that there is no significant variation in the Mulliken populations of copper upon benzene co-ordination, the change in the d_{xz} and d_{yz} orbital populations being due only to symmetry lowering. From Table 4 it can be also seen that there is no charge transfer between the copper fragment and the

Table 3 Total energies ($E_{\text{h}} \approx 4.36 \times 10^{-18} \text{ J}$) of the investigated systems

Compound	Geometry	Energy/ E_{h}
$[\text{Cu}(\text{OH})_2(\text{NH}_3)_2(\text{C}_6\text{H}_6)]$	Parallel ^a	-2132.482 64
	Bent ^b	-2132.492 85
$[\text{Cu}(\text{OH})_2(\text{NH}_3)_2]$	Fixed ^c	-1901.838 49
	Optimized	-1901.846 94
C_6H_6	Fixed ^c	-230.639 10
	Optimized	-230.641 66

^a Benzene plane parallel to the basal plane. ^b Optimized geometry as specified in the text. ^c Geometry as in the complex.

Table 4 Mulliken populations (electronic units) of the investigated systems and calculated changes in parentheses



	[Cu(OH) ₂ (NH ₃) ₂] + C ₆ H ₆	[Cu(OH) ₂ (NH ₃) ₂ (C ₆ H ₆)]
Cu	27.61	27.57 (-0.04)
Cu s	6.27	6.25 (-0.02)
Cu p	12.18	12.17 (-0.01)
p _x	4.03	4.04 (+0.01)
p _y	4.08	4.06 (-0.02)
p _z	4.07	4.07 (-)
Cu d	9.16	9.15 (-0.01)
d _{x²-y²}	2.00	2.00 (-)
d _{z²}	2.01	2.01 (-)
d _{xy}	2.00	2.00 (-)
d _{xz}	2.00	1.65 (-0.35)
d _{yz}	1.15	1.48 (+0.33)
OH	9.77	9.80 (+0.03)
NH ₃	9.92	9.93 (+0.01)
C ₆ H ₆	42.00	41.98 (-0.02)
C ¹	6.19	6.28 (+0.09)
C ²	6.19	6.24 (+0.05)
C ³	6.19	6.22 (+0.03)
C ⁴	6.19	6.21 (+0.02)
H ¹	0.81	0.63 (-0.18)
H ²	0.81	0.75 (-0.06)
H ³	0.81	0.81 (-)
H ⁴	0.81	0.81 (-)

aromatic ring, as expected due to the large distance between these two species. However, there is a polarization of the electron density of the benzene molecule, particularly the increased acidity of the hydrogen atom closest to the OH⁻ ligands. This effect contributes to the strength of the interaction and explains the spatial orientation of the C₆H₆ ligand.

Summarizing the results of our calculations, we conclude that there is a stacking interaction between the aromatic ring and the copper centre due to an electrostatic attraction. This has been evidenced both experimentally^{10,14-16,18,23} and theoretically^{16,26} in other copper(II) complexes where the axial site, pointing towards the aromatic system, is not occupied. The presence of a ligand in this site implies a steric hindrance which inhibits the stacking interaction between the aromatic group and the copper atom. This is true of complexes **1** and **2** which both have an apical ligand on the same side of the aromatic ring.

Experimental

Preparation

Complexes **1** and **2** were prepared according to the following procedures. Copper(II) nitrate (8 mmol) and the dipeptide (L-Leu-L-Phe or L-Leu-D-Phe) (8 mmol) were dissolved in water and the solution adjusted to pH 6.0 with a dilute solution of KOH. The mixture was gently heated, changing from blue to deep blue. It was concentrated and the crystals which separated upon standing at room temperature were collected, washed with aqueous ethanol and recrystallized from an aqueous solution in order to give the corresponding complexes

Table 5 Crystallographic data and details of refinement for complexes **1** and **2**

	1	2
Formula	C ₁₅ H ₂₁ CuN ₂ O ₃ ·2H ₂ O	C ₁₅ H ₂₁ CuN ₂ O ₃
<i>M</i>	376.92	340.89
Crystal dimensions/mm	0.30 × 0.05 × 0.50	0.20 × 0.15 × 0.40
Crystal system	Monoclinic	Orthorhombic
Space group	<i>P</i> 2 ₁ (no.4)	<i>P</i> 2 ₁ 2 ₁ 2 ₁ (no.19)
<i>a</i> /Å	9.393(1)	5.397(2)
<i>b</i> /Å	9.278(3)	9.190(2)
<i>c</i> /Å	10.057(2)	30.546(8)
β/°	103.98(1)	
<i>U</i> /Å ³	850.5(3)	1515.0(8)
<i>D_c</i> /g cm ⁻³	1.47	1.49
<i>Z</i>	2	4
μ(Mo-Kα)/cm ⁻¹	13.1	14.5
<i>F</i> (000)	396	712
2θ _{max} /°	60	60
Ocaltans collected	± <i>h</i> , ± <i>k</i> , ± <i>l</i>	± <i>h</i> , ± <i>k</i> , ± <i>l</i>
No. measured reflections	2742	2586
No. independent reflections	2374	1704
[<i>I</i> ≥ 3σ(<i>I</i>)]		
No. variables	207	190
<i>R</i> (<i>F_o</i>)	0.034	0.040
<i>R'</i> (<i>F_o</i>)	0.042	0.042

[CuL(H₂O)]·H₂O **1** (H₂L = L-Leu-D-Phe) and [CuL] **2** (H₂L = L-Leu-L-Phe).

Spectral measurements

Electronic spectra were recorded on a Perkin-Elmer 330 spectrophotometer in quartz cells with a path length of 10 mm. Samples were prepared by dissolving the isolated copper(II) complexes at neutral pH. The CD spectra were measured with a JASCO J-600 spectropolarimeter in quartz cells with a path length of 10 mm. Samples were prepared by dissolving the isolated copper(II) complexes in water, the concentration being 0.5 mmol dm⁻³ with respect to Cu^{II}.

Crystallography

Unit-cell dimensions were determined from Weissenberg and precession photographs, later refined by least-squares treatment of 25 reflections in the range θ 14–20°. Measurements were carried out at room temperature using the ω–2θ scan technique on a CAD4 Enraf-Nonius single-crystal diffractometer equipped with graphite monochromator and Mo-Kα radiation (λ = 0.710 73 Å). Three standard reflections, measured at regular intervals throughout the data collections, showed no noticeable variation in intensity for either crystal. Reflections having intensities *I* > 3σ(*I*) were corrected for Lorentz-polarization factors, but not for absorption, because of the small size of the crystals and the low value of μ (Table 5).

Both the structures were solved by conventional Patterson and Fourier analyses and refined (on *F*) by full-matrix least-squares calculations. All hydrogen atoms, except those of the two water molecules in **1**, were observed and introduced at calculated fixed positions (*B* = 5.0 Å²) in the final refinements. The weighting scheme²⁷ *w* = 1/[σ(*F_o*)² + (0.01*F_o*)² + 3.0] gave satisfactory results for both structures. The absolute configuration was confirmed by refining the opposite enantiomer.

Atomic scattering factors were those of ref. 28. All calculations were carried out on a MicroVAX 2000 computer, using the SDP programs.²⁹

Atomic coordinates, thermal parameters, and bond lengths and angles have been deposited at the Cambridge Crystallographic Data Centre (CCDC). See Instructions for Authors,

J. Chem. Soc., Dalton Trans., 1996, Issue 1. Any request to the CCDC for this material should quote the full literature citation and the reference number 186/137.

Computational details

Basis sets. The s,p basis for copper was taken from the (12s, 6p, 4d) set of ref. 30, with the addition of two basis functions to describe the 4p orbital,³¹ while the outermost diffuse s function was deleted. The copper d basis was the reoptimized (5d) set of ref. 32 contracted (4/1). This leads to an (11s, 8p, 5d) primitive basis for copper, contracted (8s, 6p, 2d). A (9s, 5p)/[3s, 2p] contraction was used for carbon, nitrogen and oxygen.³³ This was augmented for nitrogen and oxygen with the addition of a diffuse p function, provided in ref. 33, for the description of negative ions. The (4s)/[2s] basis of Dunning and Hay³³ was used for hydrogen, with a scale factor of 1.2.

Preliminary calculations were performed using a smaller basis set, derived for copper from Huzinaga's MINI-4 basis set,³⁴ with splitting of the outermost d function and with the addition of a p polarization function, exponent 0.096.³⁴ The MINI-1 basis set³⁵ was used for all other atoms. This basis was rejected since the basis-set superposition error³⁶ was larger than 40 kJ mol⁻¹.

Geometries and geometry optimization. The structure of [Cu(OH)₂(NH₃)₂(C₆H₆)] (see Table 4) can be viewed as a square-base pyramid with the benzene molecule at the apex. The two OH⁻ and the two NH₃ are in *cis* position at a distance of 2.0 Å from copper. The bond angles are fixed at 90°. The experimental geometries of the free molecules³⁷ were used for NH₃ and OH⁻. The Cu–O–H angle is taken to be 139.5°, having been deduced from previous calculations.³⁸ The copper atom is displaced 0.2 Å from the basal plane towards the aromatic ring, as experimentally observed. The centroid of the benzene molecule is placed above the copper atom: the distance between the copper atom and the centroid and the angle between the basal plane and that plane of the aromatic ring have been optimized. The geometry of C₆H₆ interacting with the copper fragment has been taken as equal to that experimentally observed in benzene–transition metal complexes,³⁹ while that of free C₆H₆ has been optimized. The geometry of the Cu(OH)₂(NH₃)₂ fragment has been taken as equal to that in the complex, with the copper atom in the basal plane. The simplified model used in the calculations does not consider the presence of the fifth axial ligand located on the side of the phenyl group.

Methods. The linear combination of atomic orbitals–self consistent field–molecular orbital (LCAO-SCF-MO) scheme was employed to derive the ground-state energies and wavefunctions and to perform the geometry optimizations for all the investigated systems. A doublet state with a d⁹ configuration has been assumed for all copper systems, since the ground state of Cu²⁺, ²D(3d⁹), is much lower in energy than the first ⁴D(4s¹3d⁸) excited state.

All calculations were performed on the CINECA (Centro di Calcolo Interuniversitario dell'Italia Nord Orientale) computing centre's CRAY Y-MP computer using the GAMESS-UK program system.⁴⁰

Acknowledgements

This work was partially supported by the Consiglio Nazionale delle Ricerche, Progetto Finalizzato Chimica Fine II (Rome). We thank T. Campagna for technical assistance.

References

- 1 L. D. Pettit and R. J. W. Hefford, in *Metal Ions in Biological Systems*, ed. H. Sigel, Marcel Dekker, New York, 1979, vol. 9, p. 174.
- 2 R. P. Bonomo, R. Cali, V. Cucinotta, G. Impellizzeri and E. Rizzarelli, *Inorg. Chem.*, 1986, **25**, 1641.
- 3 R. P. Bonomo, G. Maccarrone, E. Rizzarelli and M. Vidali, *Inorg. Chem.*, 1987, **26**, 2893.
- 4 V. Cucinotta, R. Purrello and E. Rizzarelli, *Comments Inorg. Chem.*, 1990, **11**, 85.
- 5 T. Sugimori, K. Shibakawa, H. Masuda, A. Odani and O. Yamauchi, *Inorg. Chem.*, 1993, **32**, 4951.
- 6 W. L. Kwik, K. P. Aug and G. I. Chen, *J. Inorg. Nucl. Chem.*, 1980, **42**, 303.
- 7 P. I. Vestues and R. B. Martin, *J. Am. Chem. Soc.*, 1980, **102**, 7906.
- 8 S. H. Kim and R. B. Martin, *J. Am. Chem. Soc.*, 1984, **106**, 1707.
- 9 O. Yamauchi, K. Tsujide and A. Odani, *J. Am. Chem. Soc.*, 1985, **107**, 659.
- 10 H. Masuda, T. Sugimori, A. Odani and O. Yamauchi, *Inorg. Chim. Acta*, 1991, **180**, 73.
- 11 O. Sinanoglu, *Int. J. Quantum Chem.*, 1980, **18**, 381.
- 12 A. Ben-Naim, *Hydrophobic Interactions*, Plenum, New York, 1980.
- 13 D. A. Dougherty, *Science*, 1996, **271**, 163.
- 14 D. van der Helm and C. E. Tatch, *Acta Crystallogr., Sect. B*, 1972, **28**, 2307.
- 15 W. A. Franks and D. van der Helm, *Acta Crystallogr., Sect. B*, 1970, **27**, 1299.
- 16 H. Masuda, O. Matsumoto, A. Odani and O. Yamauchi, *Nippon Kagaku Kaishi*, 1988, **5**, 783.
- 17 M. B. Hursthouse, S. A. A. Jayaweera, H. Milburn and A. Quick, *J. Chem. Soc., Dalton Trans.*, 1975, 2569.
- 18 H. Masuda, A. Odani and O. Yamauchi, *Inorg. Chem.*, 1989, **28**, 624.
- 19 D. van der Helm, S. E. Ealick and J. E. Burks, *Acta Crystallogr., Sect. B*, 1975, **31**, 1013.
- 20 H. Sigel and R. B. Martin, *Chem. Rev.*, 1982, **82**, 385.
- 21 C. K. Johnson, ORTEP, Report ORNL-5138, Oak Ridge National Laboratory, Oak Ridge, TN, 1976.
- 22 H. C. Freeman, *Adv. Protein Chem.*, 1967, **22**, 257.
- 23 O. Yamauchi, A. Odani, T. Kohzuma, H. Masuda, K. Toriumi and K. Saito, *Inorg. Chem.*, 1989, **28**, 4066 and refs. therein.
- 24 A. Mosset and J.-J. Bonnet, *Acta Crystallogr., Sect. B*, 1977, **33**, 2807.
- 25 B. Radomska, M. Kubiak, T. Glowiak, H. Kozlowski and T. Kiss, *Inorg. Chim. Acta*, 1989, **159**, 111.
- 26 H. Masuda, N. Fukushima, T. Sugimori and O. Yamauchi, *J. Inorg. Biochem.*, 1993, **51**, 158.
- 27 R. C. Killean and J. L. Lawrence, *Acta Crystallogr., Sect. B*, 1969, **25**, 1750.
- 28 *International Tables of Crystallography*, Kynoch Press, Birmingham, 1974, vol. 4.
- 29 B. A. Frenz, SDP, Structure Determination Package, Enraf-Nonius, Delft, 1980.
- 30 R. Roos, A. Veillard and G. Vinot, *Theor. Chim. Acta*, 1971, **20**, 1.
- 31 D. M. Hood, R. M. Pitzer and H. F. Schaefer III, *J. Chem. Phys.*, 1979, **71**, 705.
- 32 A. K. Rappe, T. A. Smedley and W. A. Goddard III, *J. Phys. Chem.*, 1981, **85**, 2607.
- 33 T. H. Dunning, jun., and P. J. Hay, in *Modern Theoretical Chemistry*, ed. H. F. Schaefer III, Plenum, New York, 1977, vol. 3, p. 1.
- 34 H. Tatewaki, Y. Sakai and S. Huzinaga, *J. Comput. Chem.*, 1981, **2**, 778.
- 35 H. Tatewaki and S. Huzinaga, *J. Comput. Chem.*, 1980, **1**, 205.
- 36 S. F. Boys and F. Bernardi, *Mol. Phys.*, 1970, **19**, 553.
- 37 E. Sutton, *Tables of Interatomic Distances and Configurations in Molecules and Ions*, The Chemical Society, London, 1958.
- 38 I. Bertini, C. Luchinat, M. Rosi, A. Sgamellotti and F. Tarantelli, *Inorg. Chem.*, 1990, **29**, 1460.
- 39 E. Solari, C. Floriani, A. Chiesi-Villa and C. Guastini, *J. Chem. Soc., Chem. Commun.*, 1989, 1747.
- 40 M. F. Guest and P. Sherwood, *GAMESS-UK, User's Guide and Reference Manual*, SERC Daresbury Laboratory, 1992.

Received 9th April 1996; Paper 6/02405J